Düzce Üniversitesi
Teknik Bilimler Dergisi

Duzce University
Journal of Technical Sciences

https://dergipark.org.tr/tr/pub/duted

Research Article

Defects Detection at Additive Manufacturing by Convolutional Deep Learning

Reza Lotfinejad, *Asghar Zajkani**

Department of Mechanical Engineering, Faculty of Engineering, Imam Khomeini International University, Qazvin, Iran.
* **Corresponding Author:** zajkani@eng.ikiu.ac.ir

Article Info:
Received: 01/05/2024, Received in revised form: 03/06/2024, Accepted: 09/06/2024.

ABSTRACT

Additive manufacturing technologies present a wide array of benefits, including the capacity to manufacture components with complex geometric forms, reduced production expenses, minimized material usage, and time efficiency. This research constitutes a significant effort to pinpoint geometric defects and dimensional irregularities as well as surface quality imperfections in the Fused Deposition Modeling process through the development of a deep learning model utilizing multi-scale convolutional neural networks. The proposed methodology encompasses three distinct scales, each capable of identifying defects of varying dimensions. The model underwent extensive hybridizing procedures for precisely training through diverse datasets, and the training process is repeated numerous times until the desired level of accuracy was attained. A sufficiently extensive image datasets are employed to train the models, leading to the precise calibration of the network. As a result, the necessity for prolonged time and intricate computations to identify large-scale defects is eliminated. The highest validation accuracy for defect detection in this study reached 94%.

Keywords: *Additive Manufacturing, Fused Deposition Modeling, Multiscale Convolutional Neural Network, Deep Learning, Defect Detection.*

Katkı Üretiminde Evrişimsel Derin Öğrenme ile Kusur Tespiti

ÖZET

Eklemeli üretim teknolojileri, karmaşık geometrik formlara sahip bileşenleri üretme kapasitesi, azaltılmış üretim giderleri, minimum malzeme kullanımı ve zaman verimliliği dahil olmak üzere çok çeşitli avantajlar sunar. Bu araştırma, çok ölçekli evrişimsel sinir ağlarını kullanan bir derin öğrenme modelinin geliştirilmesi yoluyla Erimiş Biriktirme Modelleme sürecindeki geometrik kusurların ve boyutsal düzensizliklerin yanı sıra yüzey kalitesi kusurlarının tespit edilmesi için önemli bir çaba oluşturmaktadır. Önerilen metodoloji, her biri farklı boyutlardaki kusurları tanımlayabilen üç farklı ölçeği kapsamaktadır. Model, çeşitli veri kümeleri aracılığıyla hassas bir şekilde eğitilebilmesi için kapsamlı hibridizasyon prosedürlerinden geçirildi ve eğitim süreci, istenen doğruluk düzeyine ulaşılıncaya kadar birçok kez tekrarlandı. Modelleri eğitmek için yeterince kapsamlı bir görüntü veri kümeleri kullanılır ve bu da ağın hassas kalibrasyonuna yol açar. Sonuç olarak, büyük ölçekli kusurları tespit etmek için uzun süreye ve karmaşık hesaplamalara duyulan ihtiyaç ortadan kalkar. Bu çalışmada kusur tespiti için en yüksek doğrulama doğruluğu %94'e ulaştı.

Anahtar Kelimeler: *Eklemeli Üretim, Birleştirilmiş Biriktirme Modelleme, Çok Ölçekli Evrişimsel Sinir Ağı, Derin Öğrenme, Kusur Tespiti.*

I. INTRODUCTION

Today, the demand for systems capable of autonomous decision-making has increased significantly due to technological advancements. However, this challenge has proven to be quite formidable for humans, who have been diligently working to address it for many years. While researchers have made notable strides in automation, developing systems with the capacity for human-like logical decision-making has remained a formidable task. As a result, the emulation of neural processes has served as a source of inspiration, leading to the advancement of artificial intelligence (AI) within the scientific community. Oncurrently, given the critical importance of producing complex industrial components and the limitations of additive manufacturing (AM) in certain instances, there has been a heightened emphasis on the utilization of Machine learning (ML) for in-situ defect detecting and controlling (Gunasegaram et al., 2024; Westphal and Seitz, 2021; Qin et al., 2022). Additive printing is defined as a group of layer-by-layer manufacturing processes controlled by a CAD model (Kawalkar et al., 2022; Gibson, 2015). Despite the progress made in this field, it continues to face inherent shortcomings and deficiencies, which, despite its numerous advantages, have hindered its widespread adoption in certain industries. In essence, these limitations have restricted the application of additive printing within specific industrial sectors. Consequently, addressing these challenges has the potential to significantly expand the scope of this scientific field and offer solutions to numerous industrial problems (Jin et al., 2021). ML optimizes a performance measure by using a software platform and information that obtained in the past (Alpaydın, 2014).

It is clear that low geometric accuracy and low quality surface are ignorable defects of additive printing parts (Grasso and Colosimo, 2017). These geometric defects hindered the applications of additive printing in several industries such as aerospace and medical industries (Mahesh et al., 2004). In this case, machine learning models can identify geometric defects , measure the geometric deviation and carry out geometric error compensation (Francis and Bian, 2019; Gui et al., 2022; Feng et al., 2022). The basic CAMP-BD model using the convolutional neural network and artificial neural network was introduced to predict additive printing using big data (Francis and Bian, 2019). Decision trees (Quinlan, 1986) are a common type of machine learning algorithm for classification tools. Support vector machines are designed to deal with binary classification problems (Cortes and Vapnik, 1995), but they can also be generalized to multi-class problems (Hsu and Lin, 2002). The neural network known as convolutional neural network is designed to deal with problems with images (Krizhevsky et al., 2012). Meanwhile, regularization is a process that simplifies a machine learning model by adding information during training (Bühlmann and Van De Geer, 2011; James et al., 2023).

Petsiuk et al. have produced an 88x88 mm printing plate with 8 rows and 8 columns to serve as a reference frame for the camera. Their model includes a feature that stops printing if critical deviations are detected and applies corrective measures in G-code if the printing process can be rectified. Their research has shown that the calculated position of the camera enables a one-to-one correlation between the Euclidean points recorded in G-code or in the STL model and the planar image points captured by the camera through image transfers. Their Python-developed software analyzes the G-code from the source, segments it into layers, and partitions the extruder paths into various branches, such as the filling portion, outer layer, inner walls, and support, to effectively manage the printing process. The categorization of G-code paths depends on the software algorithm used. Discrepancies within the STL model can extend to several millimeters, rendering it unreliable for this purpose, improved this problem with G-code coordinates as a reference point for positioning (Petsiuk and Pearce, 2020).

Alternately, reinforcement learning deals with teaching how to map situations to actions to maximize the value of a numerical reward signal (Xu et al., 2018), in applications such as chess games and self-driving cars. Articles have been published regarding recent applications of machine learning in additive printing (Qi et al., 2019; Patel, 2019).

Nevertheless, the utilization of a reduced number of cameras, as long as they are capable of supporting multi-view capture, leads to a decrease in computational load, eliminates the need to synchronize two images, and reduces hardware costs. At the same time, the determination of discrepancies between the real external surface and the reference boundary lines is accomplished by employing MTM and ICP algorithms. Rui Li et al. introduced a model that involved the real-time capture of images by a camera and subsequent generation of point clouds corresponding to the printed layer. These point clouds were then compared with those generated from the 3D mesh of the original design file using the ICP method, thereby enabling the identification of differences and error values. In cases where the error value surpassed the predefined threshold, the printing process was halted. The model was trained using hemispherical defects of approximately 2 mm in diameter, which were applied to defect-free areas, and an AI algorithm was employed to compare healthy and defective segments (Li, 2022).

Petsiuk and Pearce also used a camera to record images during the printing process. In that research, each image was divided into smaller areas and cells, and a gradient histogram of directions was created for the pixels inside each cell. To improve the accuracy of the model, the generated histograms were normalized to the contrast mode by calculating a value to normalize all the cells within the block. This normalization results in better invariance for changes in brightness and shading. Each histogram bar is associated with an image gradient slope angle ranging from 0 to 180 degrees. The amount of deviation is determined by comparing the histogram of the image taken from the part being printed and the reference histogram. In this model, 70% of the deviation threshold value is considered permissible (Petsiuk and Pearce, 2022).

Ero et al. proposed a machine learning-based approach using optical tomography data to identify lack of fusion and keyhole porosity. Our method employs a self-organizing map and a custom U-Net model to predict porosity effectively across different process parameters, validated through experiments and CT scanning. This approach effectively predicts porosity caused by lack of fusion or keyhole, demonstrating its potential for in-situ monitoring and quality assurance (Ero et al., 2023).

Minetola et al. placed a camera perpendicular to the build plane. By capturing images of each layer and meticulously comparing them with reference images at the pixel level, defective layers can be identified. The slicer then generates the G-code file for standard operation based on the layer thickness and print parameters, without the need for process monitoring. Subsequently, the MATLAB program parses the G-code file, processing each line and command. It is worth noting that while this model adheres to economic principles, it may not deliver the highest levels of accuracy and speed (Minetola et al., 2022). Decker and Huang employed triangular mesh data to utilize machine learning for predicting geometric accuracy in additive printing. Specifically, the 8 predictor variables computed for each vertex on the triangular mesh facilitate a direct correlation between the predictor variables and Y deviation at each vertex. The model was trained using three shapes, while a geometrically distinct shape was employed for validation. The calculation of the distance between each corner in the triangular mesh and the scanned 3D point cloud, along with the utilization of the Iterative Closest Point (ICP) method, serves as a means to compute shape deviation. Ultimately, within the dimensional accuracy range of [-0.15, 0.15], the model achieved an accuracy rate of 83.7% (Decker and Huang, 2019).

Brion and Pattinson have made significant strides in the realm of generalizable 3D printing error detection and correction through the utilization of neural networks. Their work involved the development of an extensive dataset comprising 1.2 million images, with a focus on 192 distinct parts labeled with specific print parameters. The model captured images of the nozzle tip at predetermined intervals, considering four crucial parameters: flow rate (printing), lateral speed of extruder, vertical distance of nozzle from printing bed, and material heating temperature. Furthermore, the method facilitates the connection and control of 3D printers through a network, fostering diverse data collection and collaborative learning. Notably, the adoption of the Resnet network architecture has yielded an accuracy of 82.1% in this model (Brion and Pattinson, 2022). Huang et al. have developed a non-contact instantaneous 3D laser profilometer system for visual surface defect monitoring. In their research, the 3D point cloud is initially transformed into a 2D topographical image. Subsequently, surface defects are discerned through pixel classification using the Support Vector Machine (SVM) algorithm. Beyond identifying surface bumps and depressions, the proposed methods also accurately detect small pore defects at the pixel level. This is a significant advancement for automatic quality assessment and process control in wire arc additive manufacturing (Huang et al., 2022).

In this research, the problem of dimensional accuracy, appearance and geometry of 3D printer parts has been solved by using multi-scale deep learning method. Due to the use of multiple scales and the definition of suitable pixels of the desired scale as input image, we can achieve the appropriate dimensional and geometric accuracy. On the other hand, the definition of a comprehensive dataset, in which all the appearance and dimensional defects are taken into account, has made the accuracy of the present research reach a very suitable value. Therefore, the presented model has the ability to detect defects of printed parts with high accuracy.

II. RESEARCH METHOD

In our model has been used conv-net architecture and optimized by Keras tuner. This model has been created using the complete dataset, which consists of about 33,000 images, half of which are the image of the healthy part and the other half of the defective part.

In other words, by presenting a multi-scale model compared to the researches done by others in this field, the process of detecting defects has been done by optimizing time, according to the dimensions of the desired defect. These defects detect by DL model created that trained by strong dataset.

If this model is implemented on a 3D printer, the images received from the part being printed will be entered into this model. Then these images are passed through convolutional filters by the appropriate scale according to the size of the desired defect. The trained model detects the desired defect and stops the printing process by giving an alarm if it exceeds the considered tolerance range.

The following research introduces a multi-scale AI model designed to identify printing defects in additive manufacturing parts. The design parameters of the generated model are set by the Keras Tuner library. This model is trained by using a combination of three categories of dataset. Finally, after training, this model will be able to recognize the defects shown in Table 1.

Table 1. Types of printing defects

Type of defect	Defect
Surface Defects	surface roughness
	Stringing
	Separation of layers
	Extra bump on the surface
	Holes on the surface
Internal Defects	Low density and irregular appearance of infill
Geometrical Defects	Distortion
	Deformation

According to the desired level of accuracy in detecting defects, the corresponding input batch size is used. In this way, defects with larger dimensions would be detected in less time. Training the model to detect defects with larger dimensions will take less time.

If the software model is implemented on the Raspberry Pi board, it will imbue the 3D printer with intelligent capabilities. Subsequently, as depicted in Figure 1 and Figure 2, the camera captures images of the item being printed, and the model assesses whether it is flawed or sound. In the event of a defect, the printing process is halted.

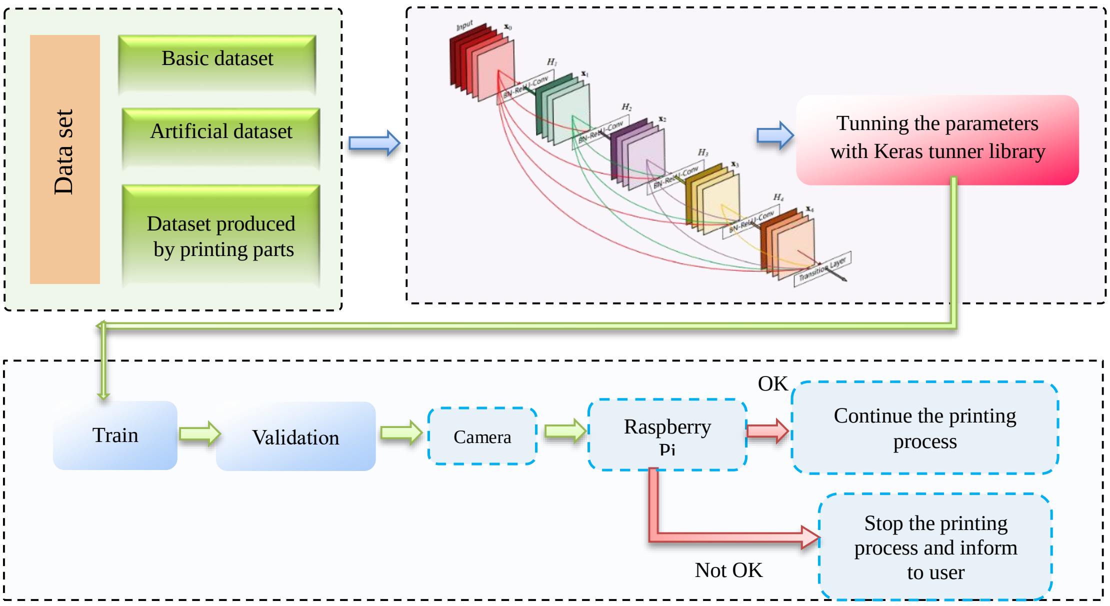

Figure 1. The overall defect detection process

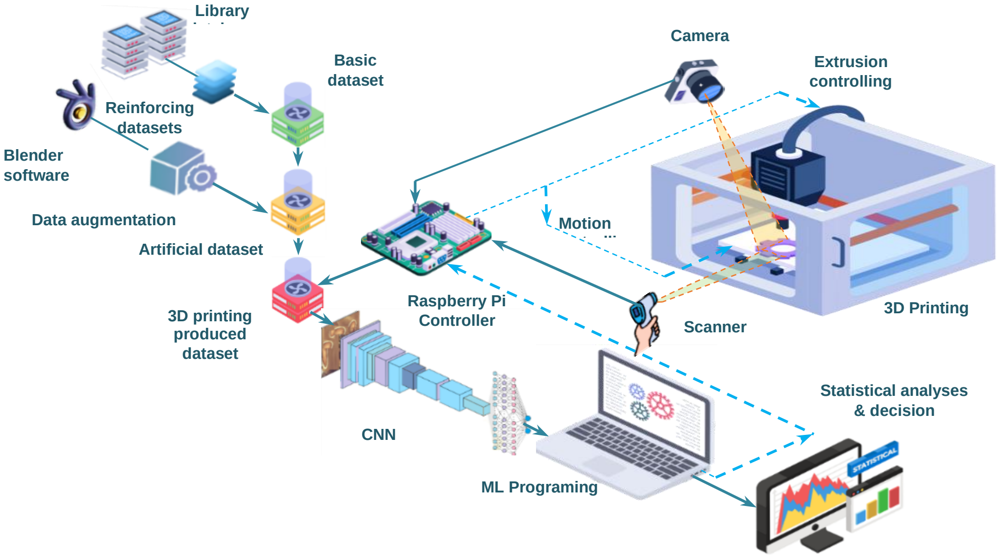

Figure 2. The illustration of defect detection process by means of a multi-scale convolutional deep learning model; dash lines in the flowchart contribute the feedback directions and controlling paths

In this study, a supercomputer was utilized for model training. The coding process involved the use of Python programming language and AI libraries such as Keras and Keras tuner for the optimal configuration of hyperparameters. The model was trained using Conv-net convolutional neural network with image dataset. Upon achieving the desired level of training and high accuracy in the validation process, the model was subsequently presented.

III. DATA SET GENERATION

The dataset comprises approximately 33,000 photos and incorporates data augmentation techniques. These methods enable the model to uphold its diagnostic performance across various conditions, while also saving time and resources. Essentially, through the implementation of these methods, a substantial dataset is generated with minimal model iterations, ensuring optimal training of the desired model. The dataset is structured into three distinct parts:

- a) Basic dataset:

It is helpful to use the dataset of research conducted by other researchers in this field. In this research, in order to make the generated dataset more powerful and to be able to recognize the model more accurately, a series of reinforcement datasets from other researches have been used [29]. This data set is shown in Figure 3.

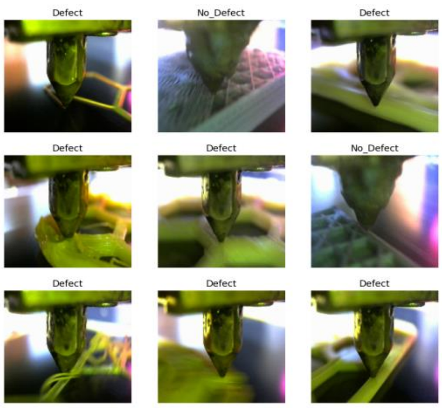

Figure 3. Basic dataset (Brion and Pattinson, 2022)

- b) Artificial dataset:

In this approach, models are constructed using sophisticated software designed for the creation of 3D models and artificial datasets. The research utilizes Blender, a widely recognized software tool that has been employed by other researchers for dataset generation. The Figure 4 shows some of these models that were created by Blender software.

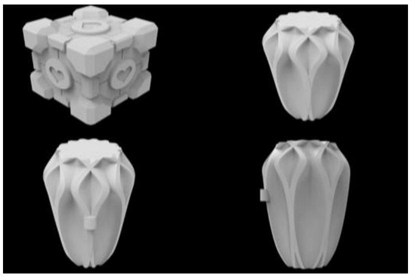

Figure 4. Some models created by the Blender software to make the data more powerful

A set of these models has been created and has made the basis of research data more powerful. Some of defects added to these models so they created the defective part of the dataset. In this way, some defects have been trained to the model.

- c) Dataset produced by printing parts:

The third portion of the generated dataset is acquired through the utilization of imaging during the printing of parts, and employing the data augmentation method to enhance the quantity of captured images shown in Figure 5.

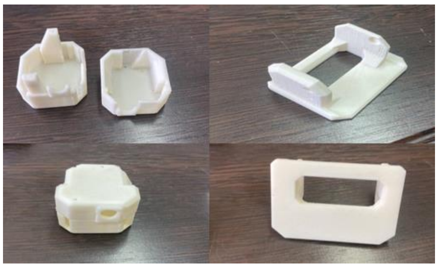

Figure 5. Some of printed parts that used for dataset generation

One of the techniques employed involves the utilization of data augmentation methods. These methods enable the model to sustain its diagnostic performance across various conditions. Furthermore, the implementation of these methods results in time and cost savings.

Multi-scale model

In this section, we will introduce multi-scale models designed to enhance detection capabilities across various scales and to reduce the computational burden of AI models. By employing filters and kernels of varying sizes, multi-scale models efficiently extract relevant features from images, irrespective of their distance from the camera frame, dimensions, and other characteristics. The model under review is segmented into three sections with input dimensions of 25x25, 75x75, and 180x180. To more accurately assess the merits of the proposed design, each scale is individually scrutinized through the calculation of accuracy metrics for defect detection.

*Model with input size of 25*25*

The smallest dimension of the filter defined in this multi-scale model is the model with the input size of 25x25. This mode is suitable for detecting errors with larger dimensions and images in which the target object is very close to the camera lens. The layering of this network in Figure 6 is shown.

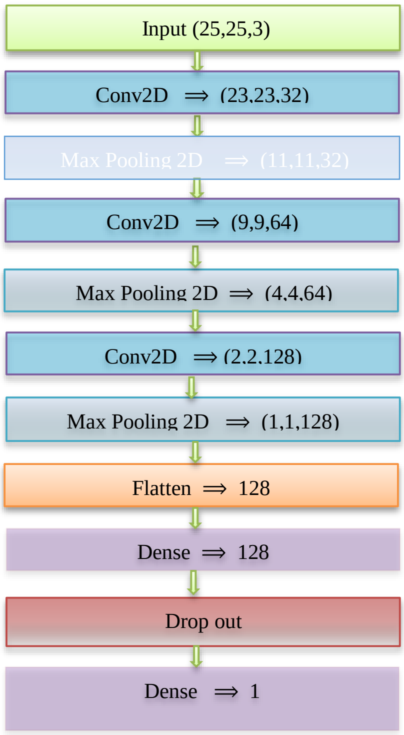

Figure 6. Network Architecture (input dimensions: 25*25)

Even though the input images and datasets contain fewer pixels in this instance, significant reductions in processing time and improved defect and object detection are observed. Consequently, the processing time for identifying defects in large objects with substantial defects is notably decreased compared to previous models. In Figure 7 the resolution of dataset images in this model are given.

Figure 7. Network resolution with an input size of 25*25

The architectural design of this model illustrates the input process, wherein an image with dimensions of 25x25 is fed into the network for processing. Subsequently, the image undergoes transformation through convolutional layers with varying kernel dimensions, resulting in a vector of size 128 within the Flatten layer. The reduction in input image size significantly decreases the computational load on the network, ultimately leading to a reduction in prediction time. This reduction in size, on the other hand, reduces the resolution of the images, so this model is suitable for detecting defects with a defined scale. Results are illustrated in Figure 8.

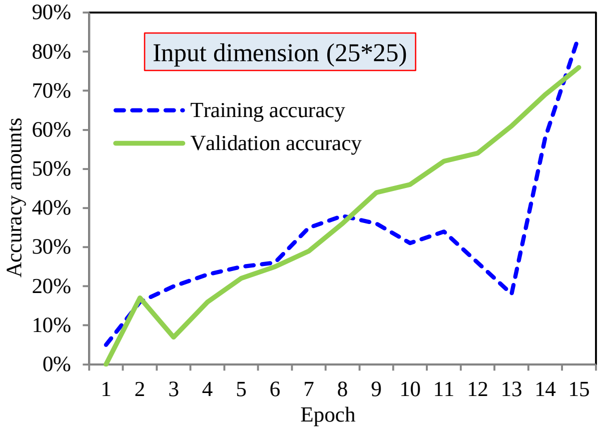

a) Accuracy prediction

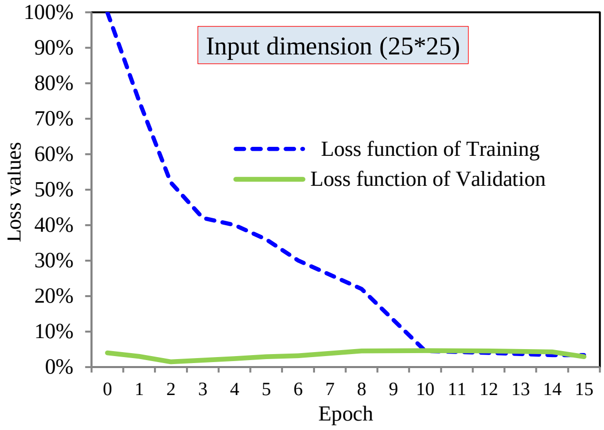

b) Loss function minimization

Figure 8. a) Accuracy and b) Loss function diagrams of multiscale model training and validation (input dimensions: 25x25)

It can be seen from the diagram in Figure 8 that:

1. The reduction in input size has facilitated the model's attainment of the appropriate stage of training during subsequent iterations.
2. The training accuracy of the model has progressively improved, reaching 37% by the seventh iteration. Subsequently, a significant surge in accuracy was observed, culminating in a remarkable 84% accuracy by the 15th iteration.
3. Notably, the validation accuracy exhibited a steep incline from the twelfth iteration, ultimately achieving a commendable 76% upon completion of network training.
4. Analysis of the training and validation error graphs reveals a marked decline in error slope during the initial three iterations, followed by stabilization at its minimum value from the fourth iteration onwards.
5. The training loss function has ultimately converged to zero, signifying a highly favorable outcome. Furthermore, the validation loss function has a notably acceptable value about 3%.

Model with input size of 75x75

The second scale defined in the presented multiscale model is characterized by an input size of 75x75. At this scale, a greater level of detail is discerned compared to the previous scale. Consequently, as processing time increases, the accuracy of defect detection also improves, enabling the identification of defects with smaller dimensions. According to the diagram in Figure 9, we can point out:

1. The accuracy of the training process has notably increased by a considerable margin up to the third iteration, reaching approximately 55%. However, a divergence becomes evident as the education process continues.
2. It is crucial to note that when the training process exhibits divergence or fluctuation in accuracy, it is imperative for the process to persist until stability is achieved in the diagram.
3. Upon attaining relative stability in the training process diagram, the process was concluded, and the model's training was finalized. Upon completion of the training process, the accuracy reached 76%, with the validation accuracy reaching 94%. This indicates the model's capability to detect defects of smaller dimensions than the 25x25 scale.

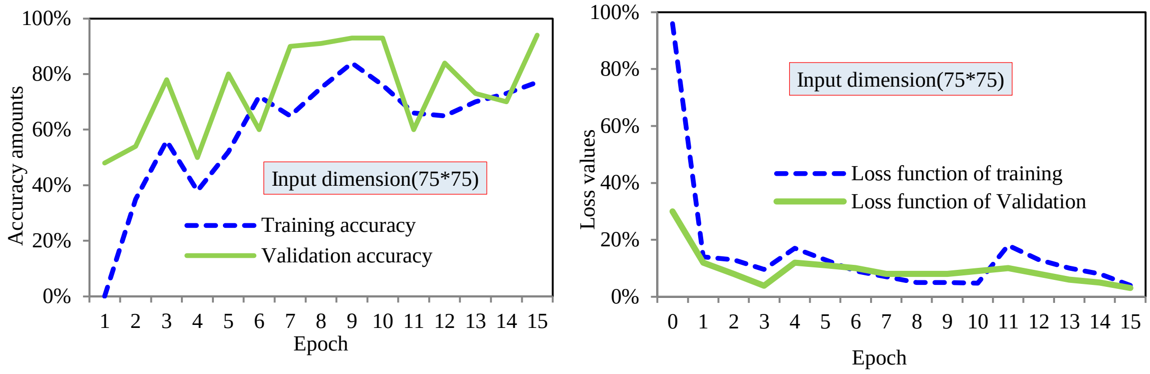

a) Accuracy prediction

b) Loss function minimization

Figure 9. a) Accuracy and b) Loss function diagrams of multiscale model training and validation (input dimensions: 75*75)

*Model with input dimensions of 180*180*

The last dimensional scale considered is the 180x180 scale. This scale also is used for one scale model and using it, comparisons are made that has been shown in Figure 10 and Figure 11.

In this model, the precision of defect detection is significantly enhanced, allowing for the detection of smaller defects. The input filter dimensions are specifically defined to detect the smallest defects in terms of geometry, dimensions, and surface quality. According to the diagram in Figure 12, it can be concluded that:

1. In the first five training repetitions, there was a sharp increase in training accuracy. From the sixth to the fifteenth repetition, this upward trend showed a more gradual slope, resulting in an 86% training accuracy.
2. The validation process's trajectory depends on the training mode. Notably, the validation accuracy exceeded the training accuracy from the sixth iteration onwards, ultimately reaching 94% accuracy.
3. Upon analyzing these graphs, it becomes clear that despite the longer processing time associated with this scale compared to smaller input batch sizes, it is well-suited for detecting smaller errors. Consequently, if the intended application is significant, the use of this approach is recommended.

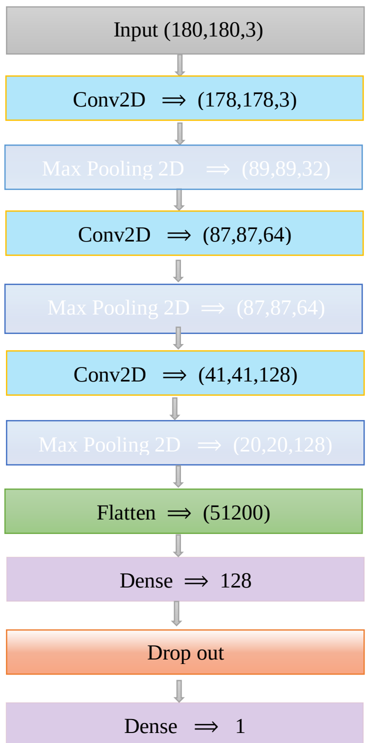

Figure 10. Network Architecture (input dimensions: 180*180)

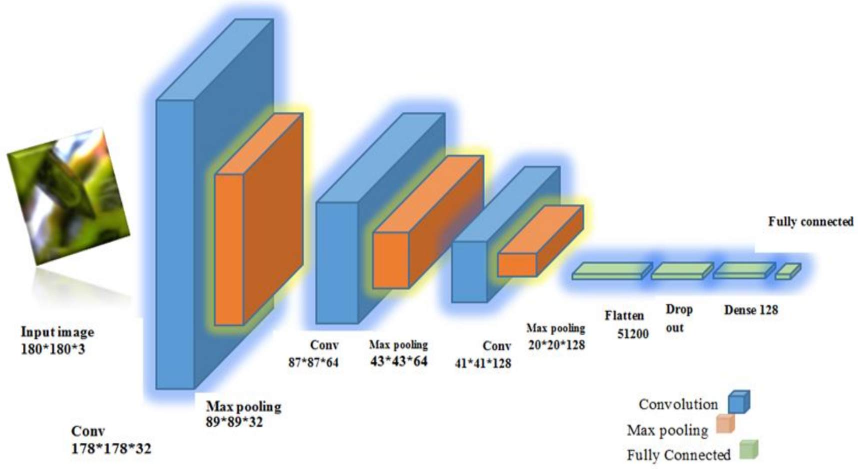

Figure 11. The CNN architecture (with input dimension 180*180)

The network resolution of this model (with input dimensions 180*180) is shown in Figure 13.

IV. Comparison of Multi-Scale and Single-Scale Models

In this section, we delve into the comparison between multi-scale and single-scale models. The comparison involves the use of charts and comparison factors of AI models, including the crucial element of time.

Based on the research, we proceed to investigate the strengths and weaknesses of the multi-scale model. Subsequently, a conclusion is drawn regarding the model's suitability for use. The advantages of employing a multi-scale model are as follows:

The presented multi-scale model can effectively utilize a scale with an appropriate input batch size based on the dimensions of the desired defect, thereby significantly reducing the time required for defect detection. This eliminates the necessity of inputting high-resolution images with specific dimensions, thus streamlining the processing and diagnosis of defects with larger dimensions.

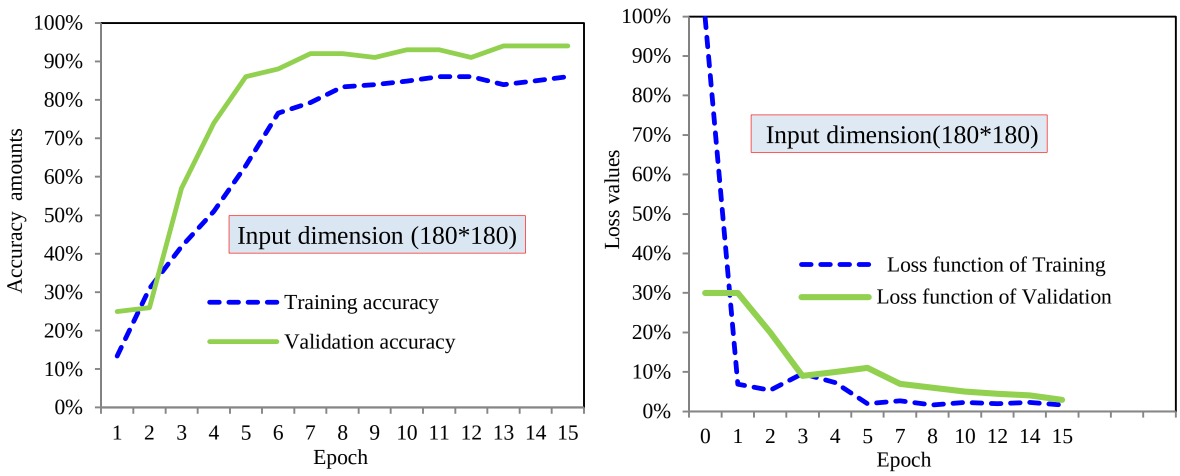

a) Accuracy prediction

b) Loss function minimization

Figure 12. a) Accuracy and b) Loss function diagrams of multiscale model training and validation (input dimensions: 180*180).

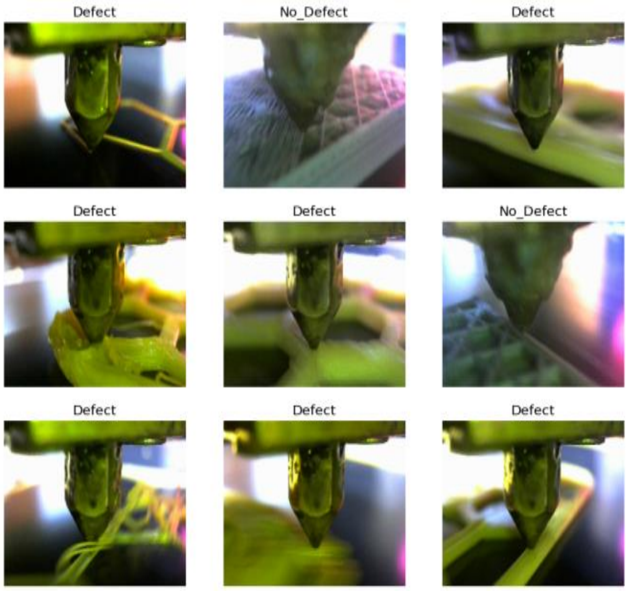

Figure 13. Network resolution of multi-scale model (input dimensions 180*180)

1. According to Table 2, the presented multi-scale model demonstrates accuracies of 76%, 93%, and 94% for scales with input batch sizes of 25x25, 75x75, and 180x180, respectively. Notably, these values correspond to the highest defect detection accuracy, with 94% accuracy matching that of the single-scale model. Consequently, the multi-scale model can achieve parity with the single-scale model in detecting small-sized defects, thereby exhibiting no weakness in this regard.
2. The multi-scale model excels in efficiently recognizing images captured at varying distances from the camera lens, a task where the single-scale model encounters processing errors due to its reliance on a single scale for all images. In contrast, the multi-scale model adeptly addresses this issue, ultimately leading to higher accuracy in predictions.

The primary concern associated with using the multi-scale model lies in identifying the correct scale. Failure to recognize the scale corresponding to the dimensions of the desired input image may lead to two potential problems:

- Selecting a model with input dimensions exceeding the optimal state results in less efficient detection and consequently, a longer processing time.
- Opting for a model with input dimensions below the optimal state poses the risk of failing to detect the desired defect.

Upon considering the aforementioned scenarios and the comparisons presented in Table 2, it becomes evident that leveraging the multi-scale model confers numerous advantages to our model, effectively contributing to optimizing the final conclusion and the time factor.

Table 2. Comparison of single-scale and multi-scale models accuracy

Model	Input batch size	Training time (hr.)	Validation accuracy	Training accuracy	Detect ability
Multi Scale	25*25, 75*75 and 180*180	2	76%	94%	Excellent
		6	93%	76%	
		11	94%	86%	
One Scale	180*180	12	94%	86%	Good

V. Conclusion

In the present study, we have employed multiscale convolutional neural networks for the purpose of defect detection in components manufactured by FDM 3D printers. Through the utilization of convolutional network training with generated datasets, the model has demonstrated the capability to identify dimensional, appearance, and surface quality defects. A multi-scale model has been implemented to identify defects of varying dimensions. The design parameters of the generated model have been established using the Keras Tuner library. Furthermore, the utilization of this model has enhanced the capacity to identify defects at varying distances from the camera lens. This model is presented across three scales: 25x25, 75x75, and 180x180. While scales with lower input dimensions exhibit reduced detection accuracy, they require significantly less time for training and diagnosing faults.

References

Alpaydın, E. (2014). *Introduction to Machine Learning, (Adaptive Computation and Machine Learning)*. almohreraladbi.

Brion, D. A., & Pattinson, S. W. (2022). Generalisable 3D printing error detection and correction via multi-head neural networks. *Nature communications*, *13*(1), 4654.

Bühlmann, P., & Van De Geer, S. (2011). *Statistics for high-dimensional data: methods, theory and applications*. Berlin, Germany: Springer Science & Business Media.

Cortes, C., & Vapnik, V. (1995). Support-vector networks. *Machine learning*, *20*, 273-297.

Decker, N., & Huang, Q. (2019, June). Geometric accuracy prediction for additive manufacturing through machine learning of triangular mesh data. In *International Manufacturing Science and Engineering Conference* (Vol. 58745, p. V001T02A043). American Society of Mechanical Engineers.

Ero, O., Taherkhani, K., & Toyserkani, E. (2023). Optical tomography and machine learning for in-situ defects detection in laser powder bed fusion: A self-organizing map and U-Net based approach. *Additive Manufacturing*, *78*, 103894.

Feng, W., Mao, Z., Yang, Y., Ma, H., Zhao, K., Qi, C., ... & Liu, S. (2022). Online defect detection method and system based on similarity of the temperature field in the melt pool. *Additive Manufacturing*, *54*, 102760.

Francis, J., & Bian, L. (2019). Deep learning for distortion prediction in laser-based additive manufacturing using big data. *Manufacturing Letters*, *20*, 10-14.

Gibson, I. G. (2015). Additive manufacturing technologies 3D printing, rapid prototyping, and direct digital manufacturing. 1–498. https://doi.org/10.1007/978-1-4939-2113-3/COVER.

Grasso, M., & Colosimo, B. M. (2017). Process defects and in situ monitoring methods in metal powder bed fusion: a review. Measurement Science and Technology, 28(4), 044005.

Gui, Y., Aoyagi, K., Bian, H., & Chiba, A. (2022). Detection, classification and prediction of internal defects from surface morphology data of metal parts fabricated by powder bed fusion type additive manufacturing using an electron beam. *Additive Manufacturing*, *54*, 102736.

Gunasegaram, D. R., Barnard, A. S., Matthews, M. J., Jared, B. H., Andreaco, A. M., Bartsch, K., & Murphy, A. B. (2024). Machine learning-assisted in-situ adaptive strategies for the control of defects and anomalies in metal additive manufacturing. *Additive Manufacturing*, 104013.

Hsu, C. W., & Lin, C. J. (2002). A comparison of methods for multiclass support vector machines. *IEEE transactions on Neural Networks*, *13*(2), 415-425.

Huang, C., Wang, G., Song, H., Li, R., & Zhang, H. (2022). Rapid surface defects detection in wire and arc additive manufacturing based on laser profilometer. *Measurement*, *189*, 110503.

James, G., Witten, D., Hastie, T., Tibshirani, R., & Taylor, J. (2023). Statistical learning. In *An Introduction to Statistical Learning: with Applications in Python* (pp. 15-67). Chamnitzer, Germany: Springer International Publishing.

Jin, Z., Zhang, Z., Ott, J., & Gu, G. X. (2021). Precise localization and semantic segmentation detection of printing conditions in fused filament fabrication technologies using machine learning. *Additive Manufacturing*, *37*, 101696.

Kawalkar, R., Dubey, H. K., & Lokhande, S. P. (2022). A review for advancements in standardization for additive manufacturing. *Materials Today: Proceedings*, *50*, 1983-1990.

Krizhevsky, A., Sutskever, I., & Hinton, G. E. (2012). Imagenet classification with deep convolutional neural networks. Advances in neural information processing systems, 25.

Li, R. (2022). Defect Detection for Additive Manufacturing with Machine Learning and Markov Decision Process.

Mahesh, M., Wong, Y. S., Fuh, J. Y. H., & Loh, H. T. (2004). Benchmarking for comparative evaluation of RP systems and processes. *Rapid Prototyping Journal*, *10*(2), 123-135.

Minetola, P., Khandpur, M. S., Iuliano, L., Calignano, F., Galati, M., & Fontana, L. (2022). In-situ monitoring for open low-cost 3D printing. In *Recent Advances in Manufacturing Engineering and Processes: Proceedings of ICMEP 2021* (pp. 49-56). Springer Singapore.

Patel, J. (2019). Data-Driven Modeling for Additive Manufacturing of Metals. *Proceedings of a ... - National Academies of Sciences, Engineering, and Medicine, Division on Engineering and Physical Sciences*.

Petsiuk, A. L., & Pearce, J. M. (2020). Open source computer vision-based layer-wise 3D printing analysis. *Additive Manufacturing*, *36*, 101473.

Petsiuk, A., & Pearce, J. M. (2022). Towards smart monitored AM: Open source in-situ layer-wise 3D printing image anomaly detection using histograms of oriented gradients and a physics-based rendering engine. *Additive Manufacturing*, *52*, 102690.

Qi, X., Chen, G., Li, Y., Cheng, X., & Li, C. (2019). Applying neural-network-based machine learning to additive manufacturing: current applications, challenges, and future perspectives. *Engineering*, *5*(4), 721-729.

Qin, J., Hu, F., Liu, Y., Witherell, P., Wang, C. C., Rosen, D. W., ... & Tang, Q. (2022). Research and application of machine learning for additive manufacturing. *Additive Manufacturing*, *52*, 102691.

Quinlan, J. R. (1986). Induction of decision trees. *Machine learning*, *1*, 81-106.

Westphal, E., & Seitz, H. (2021). A machine learning method for defect detection and visualization in selective laser sintering based on convolutional neural networks. *Additive Manufacturing*, *41*, 101965.

Xu, X., Zuo, L., Li, X., Qian, L., Ren, J., & Sun, Z. (2018). A reinforcement learning approach to autonomous decision making of intelligent vehicles on highways. *IEEE Transactions on Systems, Man, and Cybernetics: Systems*, *50*(10), 3884-3897.